J Surfact Deterg (2016) 19:645–652
DOI 10.1007/s11743-016-1796-9

SHORT COMMUNICATION

Benchmarking the Self-Assembly of Surfactin Biosurfactant at the Liquid–Air Interface to those of Synthetic Surfactants

Sagheer A. Onaizi[1,2] · M. S. Nasser[3] · Nasir M. A. Al-Lagtah[1,2]

Received: 8 September 2015 / Accepted: 11 February 2016 / Published online: 27 February 2016

Abstract The adsorption of surfactin, a lipopeptide biosurfactant, at the liquid–air interface has been investigated in this work. The maximum adsorption density and the nature and the extent of lateral interaction between the adsorbed surfactin molecules at the interface were estimated from surface tension data using the Frumkin model. The quantitative information obtained using the Frumkin model was also compared to those obtained using the Gibbs equation and the Langmuir–Szyszkowski model. Error analysis showed a better agreement between the experimental and the calculated values using the Frumkin model relative to the other two models. The adsorption of surfactin at the liquid–air interface was also compared to those of synthetic anionic, sodium dodecylbenzenesulphonate (SDBS), and nonionic, octaethylene glycol monotetradecyl ether ($C_{14}E_8$), surfactants. It has been estimated that the area occupied by a surfactin molecule at the interface is about 3- and 2.5-fold higher than those occupied by SDBS and $C_{14}E_8$ molecules, respectively. The interaction between the adsorbed molecules of the anionic biosurfactant (surfactin) was estimated to be attractive, unlike the mild repulsive interaction between the adsorbed SDBS molecules.

Keywords Adsorption · Surfactin · Biosurfactant · Synthetic surfactant · Anionic · Nonionic · Self-assembly · Liquid–air interface

Introduction

Sustainable and more environmentally-friendly technologies have been (and are still) actively sought to replace several conventional ones. For example, more clean and sustainable surface active agents (i.e., biosurfactants) have emerged as alternatives to synthetic surfactants, which are derived from polluting and unsustainable fossil fuels, in several applications [1]. Some of these bio-based surfactants have shown superior interfacial activities (e.g., reduction of interfacial tension of fluid–fluid interfaces [2, 3]) relative to synthetic ones. A recent study has also demonstrated that a detergent formulation containing biosurfactant is more effective in cleaning protein stains from solid surfaces relative to other formulations containing synthetic surfactants [4]. Additionally, a self-assembled thin film at the liquid–air interface from a binary mixture of biosurfactant–synthetic surfactant had a biosurfactant fraction that is more than 5-fold higher than its fraction in the binary mixture [5]. Thus, biosurfactants are promising surface active agents with a wide scope of industrial applications. The key obstacle for the full utilization of biosurfactants is their current high manufacturing cost, relative to the synthetic ones. However, as it is the usual case with any new technology, this limitation will be overcome in future with further advancement in the biosurfactant production and purification techniques.

In addition to the advancement in biosurfactant manufacturing technology, the full utilization of biosurfactants requires the understanding of their interfacial behavior and

✉ Sagheer A. Onaizi
sagheer.onaizi@ncl.ac.uk; sagheer.onaizi@newcastle.ac.uk

[1] School of Chemical Engineering and Advanced Materials, Newcastle University, 537 Clementi Road, #06-01, Singapore 599493, Singapore

[2] School of Chemical Engineering and Advanced Materials, Newcastle University, Newcastle upon Tyne NE1 7RU, UK

[3] Gas Processing Center, College of Engineering, Qatar University, P. O. Box 2713, Doha, Qatar

Table 1 The estimated maximum adsorption density (Γ_∞) of surfactin, SDBS and $C_{14}E_8$ and the corresponding area for each surfactant molecule at the liquid–air interface estimated using the Gibbs equation, the Langmuir–Szyszkowski and the Frumkin models

Surfactant parameter[a]	SDBS	Surfactin	$C_{14}E_8$
$\Gamma_{\infty,G}$ (μmol m^{-2})	3.19	0.97	2.67
A_G (Å^2)	52	171	62
$\Gamma_{\infty,L}$ (μmol m^{-2})	3.33	1.05	2.70
A_L (Å^2)	50	158	61.5
$\Gamma_{\infty,F}$ (μmol m^{-2})	3.67	1.16	2.84
A_F (Å^2)	45	143	58
β (−)	−0.80	2.80	−2.10

[a] The subscripts G, L and F indicate that the parameter was estimated using the Gibbs equation, the Langmuir–Szyszkowski or the Frumkin model, respectively

also the benchmarking of such behavior to that of synthetic surfactants. Such understanding and benchmarking are still greatly lacking. Thus, the aim of this study is to investigate the adsorption of surfactin, which is an interesting lipopeptide biosurfactant, at liquid–air interface; the adsorption of this biosurfactant will be compared to those of SDBS (anionic) and $C_{14}E_8$ (nonionic) synthetic surfactants. Unlike the limited number of published studies on biosurfactant adsorption, the adsorption of synthetic surfactants at different interfaces has been widely studied (see for examples [6–12]). Adsorption from synthetic surfactants [7, 13, 14] or protein-surfactant [15, 16] mixtures has been also addressed in some of the previously published studies. Additionally, a few studies have been conducted to investigate the adsorption of synthetic surfactant–biosurfactant mixtures at liquid–air interfaces [5, 17, 18]. Nonetheless, to the best of the authors' knowledge, quantitative benchmarking of biosurfactant adsorption to those of synthetic ones under the same experimental conditions has not yet been established in the literature.

The adsorption of surfactin (and the other two synthetic surfactants) takes place from solutions containing high concentrations of co- and counter-ions as such a condition is of more industrial relevance [19]. The self-assembly of these surfactants at the liquid–air interface will be followed using surface tension measurements and the obtained data will be analyzed theoretically using appropriate models to extract quantitative information on the adsorption process. Error analysis will be performed in order to assess the agreement between the computed values using the different (Frumkin, Gibbs equation and the Langmuir–Szyszkowski) models and the measured ones. Furthermore, the nature (i.e., attractive or repulsive) and also the extent of interaction between the adsorbed surfactant molecules at the liquid–air interface will be reported.

Materials and Methods

The biosurfactant, surfactin, was purchased from Wako Pure Chemical Industries Ltd (Japan). Sodium dodecylbenzenesulphonate and octaethylene glycol monotetradecyl ether were purchased from Sigma–Aldrich. Solutions of different surfactant concentrations were prepared by dissolving the surfactant of interest in 20 mM sodium phosphate buffer at pH 8. The buffer was made by dissolving the required amounts of monosodium phosphate (NaH_2PO_4) and disodium phosphate (Na_2HPO_4), which are both of analytical grade, in demineralized and purified water using a Millipore water purification system. The self-assembly of the three surface active agents at the liquid (buffer)–air interface was followed using a DSA10 tensiometer (Krüss GmbH, Hamburg, Germany). This was achieved by creating ~8 μL pendant air bubble in 8 mL of the surfactant solution of interest and then following the time-dependant reduction in the interfacial tension of the liquid–air interface until an equilibrium surface tension (γ^e) value is reached. The above procedure was repeated for other surfactant concentrations (C) in order to obtain sets of $\gamma^e - C$ data for the three surfactants. All surface tension measurements (performed in triplicate) were carried out at a fixed temperature of ~25 °C. The reproducibility of γ^e was quite high in which the variations in γ^e between the different runs at each surfactant concentration never exceeded 3 %.

The $\gamma^e - C$ data in the premicellar region were further analysed to extract quantitative information on the adsorption of the three surfactants at the liquid–air interface. The most important quantitative parameter that can be extracted from the adsorption process is the maximum adsorption density (Γ_∞). To enable the estimation of Γ_∞ from the surface tension data, the equilibrium surface tensions at different bulk concentrations of the three surface active agents in the premicellar region were regressed using different models. The simplest way to estimate Γ_∞ is to plot γ^e *versus* the logarithmic values of C up to the critical micelle concentration (CMC) of the surfactant. The slope can be used to estimate Γ_∞ according to the Gibbs adsorption isotherm shown in Eq. 1 [20, 21]:

$$\left(\frac{\partial \gamma^e}{\partial \ln C}\right)_T = -n\mathrm{RT}\,\Gamma_\infty \quad (1)$$

where T is the absolute temperature, R is the universal gas constant and n is a prefactor, which is 1 for nonionic surfactants such as $C_{14}E_8$. For ionic surfactants (e.g., surfactin and SDBS), the value of n depends on the number of species produced from the dissociation of each surfactant molecule and also on the type and concentration of the counter-ion(s) co-existing with the surfactant molecules in

the solution [22–24]. When ionic surfactants co-exist with a relatively higher concentration of the counter-ion(s), as it is the case in this study, the value of n approaches unity [10, 19, 25].

The simplicity of Eq. 1 has attracted several researchers to use it for the estimation of Γ_∞ for different surfactants adsorbing at fluid–fluid interfaces. Another model that can be used to estimate Γ_∞ from the equilibrium surface tension data is the Langmuir–Szyszkowski model [26–28] (Eq. 2), which is derived from the Gibbs equation of state coupled with the Langmuir adsorption isotherm [29–31]:

$$\gamma^e = \gamma_0 - \mathrm{RT}\,\Gamma_\infty \ln(1 + \mathrm{KC}) \tag{2}$$

where γ_0 and K are the surface tension of the solvent in the absence of surfactant and the adsorption equilibrium constant, respectively. Although the Langmuir–Szyszkowski model has been widely used to estimate Γ_∞, it does not take into account the interaction between the adsorbed molecules at the interface, which is an obvious limitation, particularly for ionic surfactants. Such a limitation is addressed by the Frumkin model [10, 32, 33] which accounts for the lateral interaction between the adsorbed molecules, shown in the coupled Eqs. 3 and 4:

$$\gamma^e = \gamma_0 + \frac{\mathrm{RT}\,\Gamma_\infty}{2}\left(2\ln(1 - \Gamma^e/\Gamma_\infty) + \beta(\Gamma^e/\Gamma_\infty)^2\right) \tag{3}$$

$$C = \frac{\Gamma^e \exp(-\beta\,\Gamma^e/\Gamma_\infty)}{K(\Gamma_\infty - \Gamma^e)} \tag{4}$$

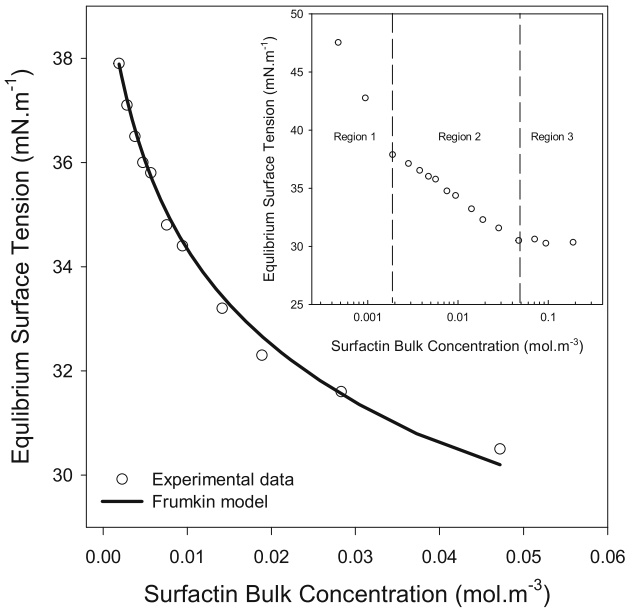

Fig. 1 Regression of surfactin $\gamma^e - C$ data in region 2 using the modified Frumkin model (the coupled Eqs. 5 and 6). The estimated maximum adsorption density (Γ_∞) and the area occupied by a surfactin molecule at the liquid–air interface are shown in Table 1. The *inset* is the plot of $\gamma^e - \ln C$ data

where Γ^e and β are the equilibrium surface coverage at a given surfactant bulk concentration and the lateral interaction parameter between the interfacially adsorbed surfactant molecules, respectively.

Results and Discussion

The Frumkin model was used to fit the premicellar $\gamma^e - C$ data of surfactin. However, the regression of the entire premicellar $\gamma^e - C$ region using the Frumkin model was quite poor (results not shown). The plot of $\gamma^e - \ln C$ (see Fig. 1 inset) has two distinct slopes in the premicellar region. Owing to the high surface activity of surfactin, the adsorption of the biosurfactant at the liquid–air interface from relatively low bulk concentrations (e.g., region 1) leads to the depletion of the biosurfactant molecules from the solution, resulting in a steep slope of the $\gamma^e - \ln C$ plot. To have reliable estimates of surfactin adsorption parameters, only $\gamma^e - C$ data in region 2 were regressed using the modified (to account for the new boundary conditions) Frumkin model shown in Eqs. 5 and 6.

$$\gamma_2^e = \gamma_{1-2}^e + \frac{\mathrm{RT}\Gamma_\infty}{2}\left(2\ln\left(\frac{\Gamma_\infty - \Gamma^e}{\Gamma_\infty - \Gamma_{1-2}^e}\right) + \beta\left(\left(\frac{\Gamma^e}{\Gamma_\infty}\right)^2 - \left(\frac{\Gamma_{1-2}^e}{\Gamma_\infty}\right)^2\right)\right) \tag{5}$$

$$C_2 = C_{1-2} + \frac{1}{K}\left(\frac{\Gamma^e \exp(-\beta\Gamma^e/\Gamma_\infty)}{\Gamma_\infty - \Gamma^e} - \frac{\Gamma_{1-2}^e \exp\left(-\beta\Gamma_{1-2}^e/\Gamma_\infty\right)}{\Gamma_\infty - \Gamma_{1-2}^e}\right) \tag{6}$$

The subscript 2 refers to the data in region 2 while the symbols γ_{1-2}^e, C_{1-2}, Γ_{1-2}^e refer to the equilibrium surface tension, surfactin bulk concentration and equilibrium surface coverage, respectively, at the intersection of region 1 and 2.

The regression of $\gamma_2^e - C_2$ data using the modified Frumkin model is shown in Fig. 1. The estimated maximum adsorption density (Γ_∞) is 1.16 μmol m^{-2}, corresponding to an area per surfactin molecule at the liquid–air interface of 143 $Å^2$. This surfactin molecular area is very similar to that (147 ± 5 $Å^2$) reported by Li *et al.* [34] for surfactin adsorption at the liquid–air interface using neutron reflectivity (NR). Shen *et al.* [35] also reported a comparable molecular area (147 and 150 $Å^2$ at pH 7.5 and 8.5, respectively) for surfactin at the liquid–air interface. Furthermore, molecular dynamic simulation studies [36, 37] reported a molecular area for surfactin monolayer at the liquid–air interface in the range of 126–170 $Å^2$. Generally, most of the published studies on surfactin adsorption at the air–water interface report a limiting molecular area ranging from 126 to 220 $Å^2$ [36, 38]. The area occupied by a surfactin molecule at the liquid–air interface reported in this work falls within this range.

In addition to the Frumkin model, surfactin $\gamma^e - C$ data in region 2 were also regressed using the Gibbs equation (Eq. 1) and a modified (after taking the change in the boundary conditions into account) Langmuir–Szyszkowski model [19]. Although the Gibbs equation and the modified Langmuir–Szyszkowski model have provided higher estimates (see Table 1) for the molecular surface area of surfactin, the deviation from the "true" measured molecular surface area obtained using neutron reflectivity is not severe, particularly for the Langmuir–Szyszkowski model. Nonetheless, the molecular surface area estimated using the Frumkin model is the closest to the one obtained using neutron reflectivity measurements. Furthermore, error analysis proved that the deviation from the measured equilibrium surface tension values is the lowest for the case of the Frumkin model (see Table 2). This further supports the superiority of the modified Frumkin model.

The regression of $\gamma_2^e - C_2$ data using the Frumkin model also provided an estimate for the lateral interaction parameter (β) between the adsorbed surfactin molecules. The estimated β value is 2.8, suggesting a net attractive interaction between the adsorbed molecules. It has been reported that the peptide ring of surfactin adopts a conformation resembling a horse saddle [1] or a ball-like structure [35]. Such a configuration might promote a strong hydrophobic interaction between the hydrophobic portions of surfactin. Screening the negative charges on the aspartic acid (Asp) and the glutamic acid (Glu) of surfactin due to the presence of high concentration (>38.5 mM) of the counter-ion (Na^+) might also play a role in reducing the electrostatic repulsive forces and bringing surfactin molecules closer to each other and thus further facilitates the hydrophobic interaction.

To compare the adsorption of this interesting anionic biosurfactant to that of synthetic anionic surfactants, SDBS adsorption at the liquid–air interface has been investigated. The equilibrium surface tension versus SDBS concentration is plotted in Fig. 2. The experimental $\gamma^e - C$ data were regressed using the Frumkin model (Eqs. 3 and 4). The estimated Γ_∞ is 3.67 μmol m^{-2}, corresponding to an area per SDBS molecule of 45 $Å^2$, which is almost one-third of that occupied by a surfactin molecule. Interestingly, the ratio of the molecular surface area of the two anionic surface active molecules at the liquid–air interface is very similar to their molecular weight ratio. However, unlike the attractive interaction between the adsorbed surfactin molecules, SDBS molecules at the interface experience a repulsive interaction ($\beta = -0.8$). Nonetheless, the low value of β indicates that the repulsion between the adsorbed SDBS molecules is relatively weak. This could be

Table 2 Error analysis

Error model [47]	Surfactin			SDBS			$C_{14}E_8$		
	Langmuir	Gibbs	Frumkin	Langmuir	Gibbs	Frumkin	Langmuir	Gibbs	Frumkin
RMSE[a] (mN/m)	0.162	0.177	0.129	0.413	0.228	0.141	0.712	0.761	0.583
SSE[b] $(mN/m)^2$	0.236	0.281	0.150	0.681	0.157	0.080	3.548	3.474	2.380
CFEF[c] (mN/m)	0.007	0.008	0.004	0.0174	0.004	0.002	0.098	0.096	0.065
MPSD[d] (mN/m)	2.16×10^{-4}	2.36×10^{-4}	1.33×10^{-4}	4.75×10^{-4}	1.34×10^{-4}	5.01×10^{-5}	0.003	0.003	0.002
ARE[e] (−)	0.034	0.039	0.032	0.045	0.023	0.015	0.110	0.109	0.086
EABS[f] (mN/m)	1.137	1.348	1.100	1.751	0.829	0.600	4.100	4.050	3.200
APE[g] (−)	0.310	0.355	0.294	0.744	0.450	0.252	1.227	1.365	0.954

[a] Residual root mean square error (RMSE) $= \sqrt{\frac{1}{n-2}\sum_i^n \left(\gamma^e_{\text{exp}} - \gamma^e_{\text{cal}}\right)^2}$

[b] Sum of the squares of the errors (SSE) $= \sum_i^n \left(\gamma^e_{\text{exp}} - \gamma^e_{\text{cal}}\right)^2$

[c] Composite fractional error function (CFEF) $= \sum_i^n \frac{\left(\gamma^e_{\text{exp}} - \gamma^e_{\text{cal}}\right)^2}{\gamma^e_{\text{exp}}}$

[d] The derivative of the Marquardt's percent standard deviation (MPSD) $= \sum_i^n \left(\frac{\gamma^e_{\text{exp}} - \gamma^e_{\text{cal}}}{\gamma^e_{\text{exp}}}\right)^2$

[e] Average relative error (ARE) $= \sum_i^n \left|\frac{\gamma^e_{\text{exp}} - \gamma^e_{\text{cal}}}{\gamma^e_{\text{exp}}}\right|$

[f] Sum of the absolute errors (EABS) $= \sum_i^n \left|\gamma^e_{\text{exp}} - \gamma^e_{\text{cal}}\right|$

[g] Average percentage errors (APE) $= \frac{\sum_i^n \left|\left(\gamma^e_{\text{exp}} - \gamma^e_{\text{cal}}\right)/\gamma^e_{\text{exp}}\right|}{n} \times 100$

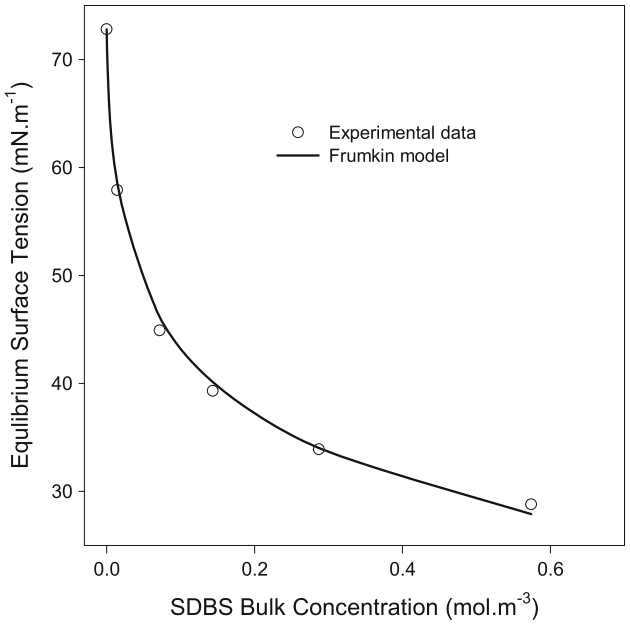

Fig. 2 Regression of SDBS $\gamma^e - C$ data using the Frumkin model (the coupled Eqs. 3 and 4). The estimated maximum adsorption density (Γ_∞) and the area occupied by an SDBS molecule at the liquid–air interface are shown in Table 1

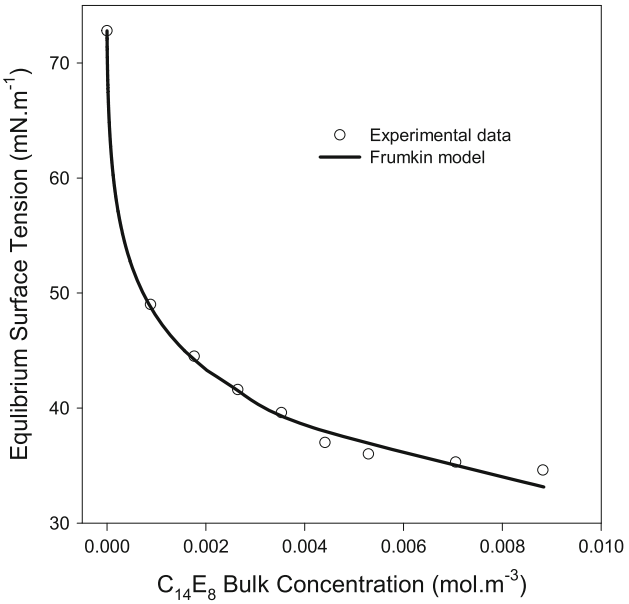

Fig. 3 Regression of $C_{14}E_8$ $\gamma^e - C$ data using the Frumkin model (the coupled Eqs. 3 and 4). The estimated maximum adsorption density (Γ_∞) and the area occupied by $C_{14}E_8$ molecule at the liquid–air interface are shown in Table 1

caused by the charge screening due to the presence of a high concentration of the counter-ion [39].

The molecular surface area of SDBS estimated using the Frumkin model is strikingly the same as that reported using NR by He *et al*. [40] for one of the SDBS isomers adsorption at the liquid–air interface. However, the molecular surface area of SDBS at the interface estimated using the Gibbs or Langmuir-Szyszkowski models (Eqs. 1 and 2) are slightly higher (52 and 50 Å^2, respectively). These molecular surface areas are close to that ($\approx$53 Å^2) reported by Zhang *et al*. [41] for SDBS adsorption at the water–air interface. Nonetheless, unlike the case of Zhang *et al*. [41] in which the adsorption of SDBS took place from water, the adsorption of SDBS under our experimental condition takes place from a solution containing a high concentration (>38.5 mM) of the counter-ion (Na^+). Since the presence of counter-ions enhances surfactant adsorption [42] (tighter packing), the molecular surface area estimated using the Frumkin model is likely more accurate. This assertion is supported by the error analysis shown in Table 2, where the Frumkin model shows better agreement (lower error) with the experimental data. Although the Frumkin model tracks the experimental data better than the other two models (based on error analysis), the differences between the molecular surface areas estimated using the three different models are not significant (see Table 1).

In addition to comparing the adsorption of surfactin to that of the synthetic anionic SDBS surfactant, its adsorption is also contrasted to that of the synthetic nonionic surfactant, $C_{14}E_8$. To enable such benchmarking, the adsorption of $C_{14}E_8$ at the liquid–air interface was studied. The equilibrium surface tensions at different bulk concentrations of the nonionic surfactant are plotted in Fig. 3. The experimental $\gamma^e - C$ data were regressed using the Frumkin model (Eqs. 3 and 4) as shown in Fig. 3. The estimated value of Γ_∞ is 2.84 μmol m^{-2}, corresponding to a molecular surface area of 58 Å^2. Lu *et al*. [43] studied the adsorption of $C_{12}E_8$ at the water–air interface using NR from the surfactant micellar solution and reported a molecular surface area of 62 ± 3 Å^2. $C_{12}E_8$ is a very close homologue (only two carbon atoms shorter) to $C_{14}E_8$ and their molecular surface areas are expected to be insignificantly different. This expectation is supported by the findings of Lu *et al*. [43] who reported no significant changes in the areas occupied by $C_{12}E_n$ at the water–air interface upon increasing the number of the ethoxy group (E) by 1 (e.g., $C_{12}E_5$ and $C_{12}E_6$).

The area occupied by a $C_{14}E_8$ molecule at the liquid–air interface is about 40 % of the area occupied by a surfactin molecule at the interface while the molecular weight ratio of surfactin to $C_{14}E_8$ is ~1.9:1. Thus, unlike the case of SDBS, the ratio of the area occupied by a $C_{14}E_8$ molecule to that occupied by a surfactin molecule deviates from the molecular weight ratio of the two surfactants.

The estimated Γ_∞ value (2.84 μmol m^{-2}) for $C_{14}E_8$ adsorption at the liquid–air interface using the Frumkin model reported in this study is close to that (2.71 μmol m^{-2}) reported by Lin *et al*. [33] who also used the same model to estimate Γ_∞ from $\gamma^e - C$ data.

However, Karakashev *et al*. [44] have reported a slightly higher Γ_∞ value (3.33 μmol m^{-2}); this value was also estimated from the regression of $\gamma^e - C$ data using the Frumkin model. Furthermore, Ueno *et al*. [20] studied the adsorption of $C_{14}E_8$ at the water–air interface and estimated a similar Γ_∞ value of 3.33 μmol m^{-2} from the $\gamma^e - C$ data using the Gibbs equation. We have also used Gibbs equation and estimated a Γ_∞ value of 2.67 μmol m^{-2}. Additionally, we have used the Langmuir-Szyszkowski model and calculated a value equivalent to 2.70 μmol m^{-2} for Γ_∞. These findings reveal that the estimated Γ_∞ values for $C_{14}E_8$ adsorption at the liquid–air interface reported in this work using the three prediction models are very close (within 6 %). Nonetheless, the Frumkin model has the lowest error, giving it a slight advantage over the Gibbs equation and the Langmuir–Szyszkowski model.

Another important parameter obtained from the regression of $\gamma^e - C$ data using the Frumkin model is the lateral interaction parameter (β) between the adsorbed $C_{14}E_8$ molecules at the interface. Since $C_{14}E_8$ molecules are neutral (uncharged), the hydrophobic attraction (positive value for β) between the $C_{14}E_8$ molecules adsorbed at the interface is expected to be significant. However, the estimated value for β is −2.1, suggesting a repulsive interaction between the adsorbed $C_{14}E_8$ molecules. Negative values for β have been also reported by other researchers for other nonionic surfactants adsorption at liquid–air interfaces [45, 46]. Such non-physical values of β have motivated Fainerman *et al*. [7] to propose that, in such cases, β might be considered as only a fitting parameter with no physical meaning.

Conclusions

The Frumkin model seems to provide a more accurate estimation of the maximum adsorption density of the biosurfactant, surfactin, as well as of the other two synthetic surfactants. The lateral interaction between the adsorbed surfactin molecules is estimated to be attractive despite the fact that surfactin carries two permanent negative charges at pH 8. Such attraction is probably promoted by the conformation of surfactin, which might have brought the hydrophobic moieties of surfactin closer to each other. Screening the negative charges on the two amino acids (Glu and Aps) of surfactin by the counter-ion (Na^+) would play a role in minimizing the Debye length and this may further enhance the hydrophobic attraction between the hydrophobic portions of the adsorbed surfactin molecules. Unlike the attractive interaction between the interfacially assembled anionic surfactin molecules, the interaction between the adsorbed anionic SDBS molecules was estimated to be repulsive. Despite the different modes of lateral interaction between the adsorbed surfactin and SDBS molecules, the ratio of the area occupied by a surfactin molecule to that occupied by an SDBS molecule is comparable to their molecular mass ratio. Such correlation, however, was not established between surfactin and the nonionic $C_{14}E_8$ surfactant.

References

1. Dexter AF, Middelberg APJ (2008) Peptides as functional surfactants. Ind Eng Chem Res 47:6391–6398
2. Arima K, Kakinuma A, Tamura G (1968) Surfactin, a crystalline peptide lipid surfactant produced by *Bacillus subtilis*: isolation, characterization and its inhibition of fibrin clot formation. Biochem Biophys Res Commun 31:488–494
3. Cooper DG, Macdonald CR, Duff SJB, Kosaric N (1981) Enhanced production of surfactin from *Bacillus subtilis* by continuous product removal and metal cation additions. Appl Environ Microbiol 42:408–412
4. Onaizi SA, He L, Middelberg APJ (2009) Rapid screening of surfactant and biosurfactant surface cleaning performance. Colloids Surf B 72:68–74
5. Onaizi SA, Nasser MS, Twaiq FA (2012) Micellization and interfacial behavior of a synthetic surfactant–biosurfactant mixture. Colloids Surf A 415:388–393
6. Gurkov TD, Dimitrova DT, Marinova KG, Bilke-Crause C, Gerber C, Ivanov IB (2005) Ionic surfactants on fluid interfaces: determination of the adsorption; role of the salt and the type of the hydrophobic phase. Colloids Surf A 261:29–38
7. Fainerman VB, Lucassen-Reynders EH, Miller R (1998) Adsorption of surfactants and proteins at fluid interfaces. Colloids Surf A 143:141–165
8. Giribabu K, Ghosh P (2007) Adsorption of nonionic surfactants at fluid–fluid interfaces: importance in the coalescence of bubbles and drops. Chem Eng Sci 62:3057–3067
9. Ma J-G, Boyd BJ, Drummond CJ (2006) Positional isomers of linear sodium dodecyl benzene sulfonate: solubility, self-assembly, and air/water interfacial activity. Langmuir 22:8646–8654
10. Onaizi SA, Nasser MS, Al-Lagtah NMA (2015) Adsorption of an anionic surfactant at air–liquid and different solid–liquid interfaces from solutions containing high counter-ion concentration. Colloid Polym Sci 293:2891–2899
11. Phan CM, Nguyen AV, Evans GM (2005) Dynamic adsorption of sodium dodecylbenzene sulphonate and Dowfroth 250 onto the air–water interface. Miner Eng 18:599–603
12. Prosser AJ, Franses EI (2001) Adsorption and surface tension of ionic surfactants at the air–water interface: review and evaluation of equilibrium models. Colloids Surf A 178:1–40
13. Zhang R, Somasundaran P (2006) Advances in adsorption of surfactants and their mixtures at solid/solution interfaces. Adv Colloid Interface Sci 123–126:213–229

14. Fainerman VB, Aksenenko EV, Mys AV, Petkov JT, Yorke J, Miller R (2010) Adsorption layer characteristics of mixed SDS/CnEOm solutions. 3. Dynamics of adsorption and surface dilational rheology of micellar solutions. Langmuir 26:2424–2429
15. He L, Onaizi SA, Dimitrijev-Dwyer M, Malcolm AS, Shen H-H, Dong C et al (2011) Comparison of positional surfactant isomers for displacement of RuBisCO protein from the air–water interface. J Colloid Interface Sci 360:617–622
16. Dan A, Gochev G, Kragel J, Aksenenko EV, Fainerman VB, Miller R (2013) Interfacial rheology of mixed layers of food proteins and surfactants. Curr Opin Colloid Interface Sci 18:302–310
17. He L, Malcolm AS, Dimitrijev M, Onaizi SA, Shen H-H, Holt SA et al (2009) Cooperative tuneable interactions between a designed peptide biosurfactant and positional isomers of SDOBS at the air–water interface. Langmuir 25:4021–4026
18. Jian H-L, Liao X-X, Zhu L-W, Zhang W-M, Jiang J-X (2011) Synergism and foaming properties in binary mixtures of a biosurfactant derived from *Camellia oleifera* Abel and synthetic surfactants. J Colloid Interface Sci 359:487–492
19. Onaizi SA, Nasser MS, Twaiq FA (2014) Adsorption and thermodynamics of biosurfactant, surfactin, monolayers at the air-buffered liquid interface. Colloid Polym Sci 292:1649–1656
20. Ueno M, Takasawa Y, Miyashige H, Tabata Y, Meguro K (1981) Effects of alkyl chain length on surface and micellar properties of octaethylene glycol-n alkyl ethers. Colloid Polym Sci 259:761–766
21. Schramm LL, Stasiuk EN, Marangoni DG (2003) Surfactants and their applications. Annu Rep Prog Chem Sect C 99:3–48
22. Li PX, Dong CC, Thomas RK, Penfold J, Wang Y (2011) Neutron reflectometry of quaternary gemini surfactants as a function of alkyl chain length: anomalies arising from ion association and premicellar aggregation. Langmuir 27:2575–2586
23. An SW, Lu JR, Thomas RK, Penfold J (1996) Apparent anomalies in surface excesses determined from neutron reflection and the Gibbs equation in anionic surfactants with particular reference to perfluorooctanoates at the air/water interface. Langmuir 12:2446–2453
24. Eastoe J, Nave S, Downer A, Paul A, Rankin A, Tribe K et al (2000) Adsorption of ionic surfactants at the air–solution interface. Langmuir 16:4511–4518
25. Onaizi SA, Nasser MS, Al-Lagtah NMA (2015) Self-assembly of a surfactin nanolayer at solid–liquid and air–liquid interfaces. Eur Biophys J. doi:10.1007/s00249-015-1099-5
26. Adamson AW (1991) Physical chemistry of surfaces, 5th edn. Wiley, New York
27. Lavi P, Marmur PA (2000) Adsorption isotherms for concentrated aqueous-organic solutions (CAOS). J Colloid Interface Sci 230:107–113
28. Rosen JM (2004) Surfactants and interfacial phenomena, 3rd edn. Wiley, New York
29. Onaizi SA, He L, Middelberg APJ (2009) Proteolytic cleaning of a surface-bound rubisco protein stain. Chem Eng Sci 64:3868–3878
30. Onaizi SA, He L, Middelberg APJ (2010) The construction, fouling and enzymatic cleaning of a textile dye surface. J Colloid Interface Sci 351:203–209
31. Onaizi SA, Nasser MS, Twaiq FA (2014) Lysozyme binding to tethered bilayer lipid membranes prepared by rapid solvent exchange and vesicle fusion methods. Eur Biophys J 43:191–198
32. Eastoe J, Dalton JS (2000) Dynamic surface tension and adsorption mechanisms of surfactants at the air–water interface. Adv Colloid Interface Sci 85:103–144
33. Lin S-Y, Lee Y-C, Shao M-J, Hsu C-T (2001) A study on surfactant adsorption kinetics: the role of the data of equation of state g(G) for $C_{14}E_8$. J Colloid Interface Sci 244:372–376
34. Li PX, Li ZX, Shen H-H, Thomas RK, Penfold J, Lu JR (2013) Application of the Gibbs equation to the adsorption of nonionic surfactants and polymers at the air–water interface: comparison with surface excesses determined directly using neutron reflectivity. Langmuir 29:9324–9334
35. Shen H-H, Lin T-W, Thomas RT, Taylor DJF, Penfold J (2011) Surfactin structures at interfaces and in solution: the effect of pH and cations. J Phys Chem B 115:4427–4435
36. Gallet X, Deleu M, Razafindralambo H, Jacques P, Thonart P, Paquot M et al (1999) Computer simulation of surfactin conformation at a hydrophobic/hydrophilic interface. Langmuir 15:2409–2413
37. Jang SS, Goddard WA III (2006) Structures and properties of newton black films characterized using molecular dynamics simulations. J Phys Chem B 110:7992–8001
38. Gang H-Z, Liu J-F, Mu B-Z (2011) Molecular dynamics study of surfactin monolayer at the air/water interface. J Phys Chem B 115:12770–12777
39. Onaizi SA, Malcolm AS, He L, Middelberg APJ (2007) Directed disassembly of an interfacial rubisco protein network. Langmuir 23:6336–6341
40. He L, Onaizi SA, Dimitrijev-Dwyer M, Malcolm AS, Shen H-H, Dong C et al (2011) Comparison of positional surfactant isomers for displacement of rubisco protein from the air–water interface. J Colloid Interface Sci 360:617–622
41. Zhang XL, Taylor DJF, Thomas RK, Penfold J (2011) The role of electrolyte and polyelectrolyte on the adsorption of the anionic surfactant, sodium dodecylbenzenesulfonate, at the air–water interface. J Colloid Interface Sci 356:656–664
42. Ghosh P (2009) Colloid and interface science. PHI Learning Private Pvt Ltd., New Delhi
43. Lu JR, Thomas RK, Penfold J (2000) Surfactant layers at the air/water interface: structure and composition. Adv Colloid Interface Sci 84:143–304
44. Karakashev S, Manev E, Nguyen A (2004) Interpretation of negative values of the interaction parameter in the adsorption equation through the effects of surface layer heterogeneity. Adv Colloid Interface Sci 112:31–36
45. Karakashev SI, Manev ED (2002) Effect of interactions between the adsorbed species on the properties of single and mixed-surfactant monolayers at the air/water interface. J Colloid Interface Sci 248:477–486
46. Karakashev SI, Manev ED (2003) Correlation in the properties of aqueous single films and foam containing a nonionic surfactant and organic/inorganic electrolytes. J Colloid Interface Sci 259:171–179
47. Hadi M, Samarghandi MR, MacKay G (2010) Equilibrium two-parameter isotherms of acid dyes sorption by activated carbons: study of residual errors. Chem Eng J 160:408–416

Sagheer A. Onaizi is currently a lecturer in Chemical Engineering at the School of Chemical Engineering and Advanced Materials, Newcastle University. He received his B.Sc. in Chemical Engineering from Jordan University of Science and Technology, M.Sc. in Chemical Engineering from Twente University, Professional Doctorate in Engineering (Process Development and Design) from Twente University, PhD in Biochemical Engineering from Queensland University, Newcastle Teaching Award in higher education and Certificate in Advanced Studies in Academic Practice from Newcastle University. He is a Fellow of The Higher Education Academy (UK) and he is also a member of a number of other professional organizations. His research expertise and interests are in the fields of wastewater treatment using biochemical processes, biomimetic, enzymatic reactions and colloidal and interfacial phenomena.

M. S. Nasser is currently an assistant professor at the Gas Processing Center (GPC), Qatar University. He received his Ph.D. from the University of Manchester, an M.Sc. from the University of Twente and a B.Sc. from Jordan University of Science and Technology, all in Chemical Engineering. His research is categorized in the following main areas: Rheology of Complex fluids, Colloidal and interfacial phenomena, and Wastewater treatment.

Nasir M. A. Al-Lagtah is currently a lecturer in Chemical Engineering at the School of Chemical Engineering and Advanced Materials, Newcastle University. He received his B.Sc. and M.Sc. from Jordan University of Science and Technology and his Ph.D. from Queen's University Belfast, all in Chemical Engineering. His research interests include further valorization of lignin residue (biorefinery byproduct) for the production of functionalized materials (catalysts, nanotubes, nanoparticles and hydrogels) for the application in the fields of energy, advanced water treatment and pharmaceutical processes; modelling and simulation of refinery and bioenergy processes using Aspen HYSYS and Aspen Plus.